JVSTB Journal of Vacuum Science & Technology B

Alkali azide based growth of high quantum efficiency photocathodes

Luca Cultrera, Mark Brown, Siddharth Karkare, William Schaff, Ivan Bazarov, and Bruce Dunham

Citation: Journal of Vacuum Science & Technology B **32**, 031211 (2014); doi: 10.1116/1.4876184
View online: http://dx.doi.org/10.1116/1.4876184
View Table of Contents: http://scitation.aip.org/content/avs/journal/jvstb/32/3?ver=pdfcov
Published by the AVS: Science & Technology of Materials, Interfaces, and Processing

Alkali azide based growth of high quantum efficiency photocathodes

Luca Cultrera,[a] Mark Brown, Siddharth Karkare, William Schaff, Ivan Bazarov, and Bruce Dunham
Cornell Laboratory for Accelerator Sciences and Education, Cornell University, Ithaca, New York 14853

(Received 11 March 2014; accepted 1 May 2014; published 13 May 2014)

The authors report on successful growth of bialkali photocathode based on CsK_2Sb using the alkali metal vapors generated by thermal decomposition of alkali azides. Details about the ultrahigh vacuum growth system and the procedure used are provided. The final quantum efficiency of the photocathode under illumination with 532 nm laser is 9.6%. This value is comparable to the largest ones obtained in our previous experiments using commercial dispensers, indicating that alkali azides are a viable alternative. © *2014 American Vacuum Society*. [http://dx.doi.org/10.1116/1.4876184]

I. INTRODUCTION

During the past decade, the scientific community has shown a renewed interest in the physics of photoemission electron sources with applications related to the generation of high brightness electron beams suitable to drive fourth generation x-ray sources such as energy recovery linacs (ERL) and free electron lasers, nuclear and high energy physics experiments (e.g., electron coolers and electron–ion colliders), as well as an electron source for ultrafast electron diffraction experiments.[1]

Many different photosensitive materials are widely used in photon detection and imaging devices such as photomultiplier tubes and night vision cameras. The use of alkali antimonides photocathode materials in an RF gun based photoinjector was already reported in 1995,[2] but important properties such as mean transverse energy (MTE), their response time, and the lifetime of photocathode materials when operated in modern photoinjector or dedicated devices have been systematically measured only in recent years.[3–7] Some aspects related to the physics of photoemission are not yet completely understood, and for this reason, Cornell University has launched a dedicated effort with the goal of investigating and optimizing properties of photocathode materials. Part of the work is dedicated to developing reliable growth procedures for synthesizing alkali antimonide photocathode materials with characteristics suitable for operation in high average power, high brightness photoinjectors.[8] Results related to the growth and characterization of high quantum efficiency (QE) photocathodes operated in the ERL injector prototype in use at Cornell University have been reported, showing that high quantum efficiency alkali antimonides not only provide electron beams with MTE similar to the one obtained from GaAs activated to negative electron affinity but also offer enhanced ruggedness with respect to vacuum conditions, resulting in longer lifetime when operating at very high average current levels.[9] Alkali antimonide photocathodes based on Cs_3Sb, CsK_2Sb, and Na_2KSb materials are routinely grown for the ERL photoinjector prototype. QEs in the range of 10% have been achieved at 520 nm incident light wavelength, the operating wavelength typical of high current photoinjector drive lasers.[10]

One of the main limitations in the reproducibility of the growth procedures is related to an intrinsic unreliability of the dispensers used to generate alkali vapors during the growth of antimonide-based photocathodes. Commercially available alkali metal vapor dispensers are available using either alkali metal chromates[11] or bismuth alloys.[12] The best results in terms of quantum efficiency achieved so far have been obtained from the bismuth alloys-based dispensers. Such dispensers hold larger quantities of alkali metal as compared to alkali metal chromate dispenser and are able to provide larger atomic fluxes. On the other hand, they present the drawback of reactivity with oxygen containing species. For this reason, an indium-based seal is employed to keep the alloy under an inert atmosphere. Once the seal is broken under vacuum, the dispenser cannot be exposed to open air; otherwise, the alloy will be oxidized and permanently contaminated. Furthermore, as the atomic ratio between Bi and the alkali metal changes because of the continuous use of the dispenser, the operating parameters must be adjusted to reproduce the same experimental conditions. In the worst case scenario, Bi can also evaporate from the dispenser contaminating the sample.

Possible obvious alternatives to the use of alkali chromate or bismuth alloy-based dispensers are represented by pure alkali metals and alkali azides. The use of pure metal based sources has been already proven to be effective in yielding photocathodes with quantum efficiency comparable to the ones grown in sealed tubes,[13] but the handling of pure metals has to be performed in inert gas atmosphere because of the well-known reactivity of alkali metal in their pure state. On the other hand, alkali azides are stable compounds in air (chemical formula AN_3, were A is the alkali metal) and are known to decompose at moderate temperatures,[14–16] releasing high purity alkali metals vapors and nitrogen gas, the latter being inert and not expected to be harmful to the photoemissive properties of the cathode. Depletion of the AN_3 from the crucible will not result in the release of any potential contaminants. Moreover, alkali azides can be reused after the system has been vented without any detectable effect on the final properties of grown photocathode.

Here, we report on the experimental setup and procedure used for growth of CsK_2Sb material having quantum efficiencies close to 10% at 532 nm showing that alkali azides are an effective alternative to commercially available sources for the synthesis of alkali antimonide-based photocathodes. The

[a]Electronic mail: lc572@cornell.edu

growth system and procedures described herein can be scaled up for the purpose of growing photoemissive materials over large area substrates for application in high energy physics experiments involving single photon detection.

II. EXPERIMENTAL SET UP

The UHV growth system designed with the purpose of using alkali azides as sources of high purity alkali metals vapors for the growth of high QE cathodes consists of a vacuum chamber equipped with four furnaces for the evaporation of metals, a substrate heater, and a quartz microbalance to measure the atomic fluxes. Because of the different sticking coefficient of the different alkali atomic species to the substrate and to quartz microbalance crystals surfaces, the quantitative determination of the flux as measured by the frequency shift of the microbalance crystal can be used only as reference to compare different procedures and to evaluate the stability of the flux generated by azides thermal decomposition.

The substrate holder is electrically insulated and is radiatively heated with an electrical heating element placed a few millimeters from the back of the substrate. The substrate is directly connected to a thermocouple to measure its surface temperature. In order to measure the photocurrent, the substrate is biased negatively with respect to the chamber walls to collect the electrons emitted while illuminating the cathode with a laser. The use of a lock-in amplifier and a mechanical chopper to modulate the laser light intensity allows further increasing the signal to noise ratio and to remove unwanted DC components from the photocurrent signal. During preliminary experiments, the photocurrent flowing out of the substrate depended on the vacuum pressure if a bias larger then few tens of volts was used. This is attributed to the increase of the electron impact ionization cross section, which leads to a larger ion content in the residual gas in the vicinity of the photocathode surface. Since the substrate is negatively biased, the ions generated by photoelectrons will be collected by the substrate, in addition to the measured value of the current due to photoelectrons. In order to mitigate this effect a low voltage of -18 V was used to bias the substrate. A schematic of the growth system is provided in Fig. 1.

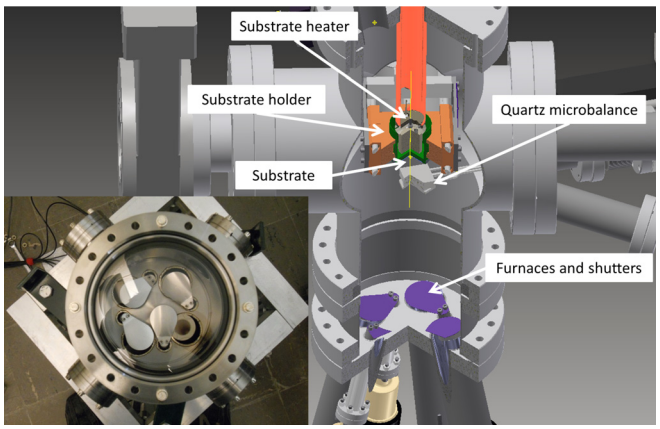

FIG. 1. (Color online) Schematic of the growth chamber assembly and a picture showing the flange hosting the furnaces and shutters.

The pumping system has been designed to minimize the contamination of the samples during the growth over a wide range of pressures from 10^{-2} down to 10^{-8} Pa levels. When alkali azides temperature is raised to 300 °C, the molecular bonds are broken, resulting in a release of high purity alkali metals and nitrogen gas.[14–16] In order to achieve fluxes compatible with the growth of alkali antimonides, a vacuum level in the range of 10^{-3} Pa must be supported by the pumping system.

This continuous gas load cannot be easily handled by an ion pump. At such high vacuum levels, the sputtering rates generated by the plasma forming in the vicinity of ion pump electrodes can induce the release of large quantities of chemical elements and molecules that can quickly poison the cathode surface. For this reason, a turbomolecular pump was connected to our chamber through a gate valve to support or replace the ion pump in maintaining the vacuum once the pressure becomes too high to be compatible with the ion pump.

The sources of metal vapors are based on Varian Molecular Beam Epitaxy furnaces (Mod. 981-4134) hosting a 16cc high purity BN crucible. Each furnace is equipped with a shutter operated by a rotary pneumatic actuator. Preliminary experiments revealed that when temperature of the furnaces is raised high enough to promote dissociation of the alkali azide, a solid to liquid transition can occur and the liquid will start to boil, generating a large number of macroscopic droplets that deposit on the substrate. In order to avoid droplet ejection from the boiling material contained in the crucible, a special mask was designed to remove direct line-of-sight between the alkali azide and the substrate surface. The mask has been designed so that can be hooked to the BN crucible lip by means of six small tabs. Another beneficial effect of the mask is an improved thermal stability of the furnace with respect to the shutter position. When the mask was not used, we observed furnace temperature drifts of 15 °C when the shutter was moved from open to closed position as a result of the thermal shielding change induced by the shutter position. Figure 2 shows pictures of one of the shielding mask before and after being connected to the BN crucible lip.

The bottom flange of the deposition chamber is equipped with four furnaces allowing evaporating Sb (from Alfa-Aesar 99.9999% purity beads), Cs (from Sigma-Aldrich CsN_3 99.99% purity), K (from Sigma-Aldrich $KN_3 > 99.9\%$ purity), and Na (from Sigma-Aldrich $NaN_3 > 99.5\%$ purity). Due to the limited space available and to avoid mechanical interference of the shutters, the evaporation of different chemical species can occur only in sequence (i.e., no codeposition of different elements could be performed). The four furnaces are installed so that the intersection of their symmetry axis coincides with the center of the substrate, which is placed about 20 cm from the mouth of each crucible.

III. RESULTS

The substrates used for growth procedures described here are stainless steel substrates polished with diamond paste to a mirror finish. The smallest diamond grain size used for the

FIG. 2. (Color online) Details of the insets used to avoid direct line of sight between the azides in the crucibles and the substrate where growth is occurring.

polishing was 100 nm. After a 24 h bake at 150 °C, the chamber vacuum level was 2×10^{-7} Pa. Before attempting film growth, the furnaces and the substrate were extensively degassed by keeping the substrate at 550 °C and the furnaces at 160 °C for 24 h. At the end of this procedure, the vacuum level, with the puck at 550 °C, was of 2×10^{-6} Pa.

The source temperatures were set to 100 °C [see Fig. 3(a)] and substrate heater was turned off to allowing the polished stainless steel surface to cool down as reported in figure [see Fig. 3(c)]. The Sb furnace temperature was ramped to 400 °C. After 40 min the substrate temperature lowered to 200 °C. The temperature of the Sb source was then increased to 515 °C and the shutter was opened. The Sb flux obtained from the quartz microbalance placed in the vicinity of the substrate was measured to be 3×10^{13} atoms/cm^2 s and is reported in Fig. 3(b). The initial observed transient was

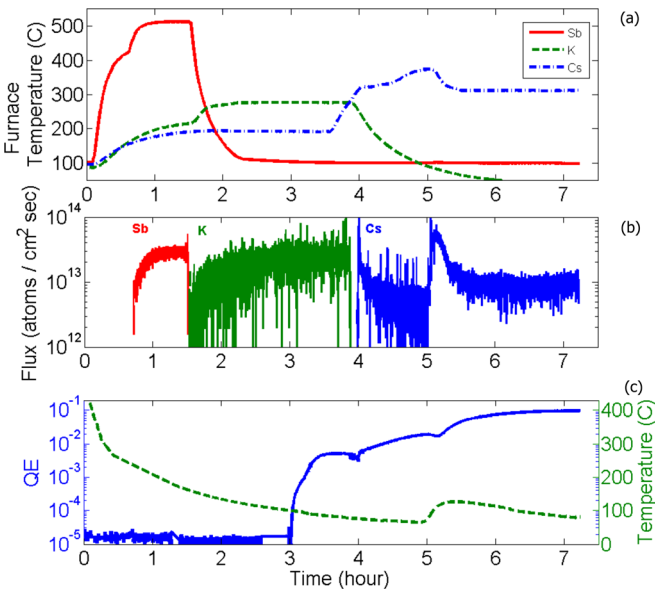

FIG. 3. (Color online) (a) Temperatures of furnaces hosting Sb, KN_3, and CsN_3; (b) Atomic fluxes at the substrate surface as deduced by frequency shift of the quartz microbalance crystal; (c) Substrate temperature and QE at 532 nm of the photocathode as measured during the growth process.

related to the not yet stabilized temperature of the furnace. Using the deposition rate inferred from the quartz microbalance, the Sb layer thickness grown was limited at 20 nm by closing the furnace shutter and then by decreasing the operating temperature of the furnace to 100 °C. During the growth of the Sb layer, the temperature of the furnace hosting KN_3 was raised to 200 °C and, as the Sb layer was approaching the final thickness of 20 nm, the heater current was set to increase the temperature of the KN_3 furnace to 275 °C. When the shutter of the KN_3 furnace was opened allowing the K flux to reach the substrate, the temperature of the furnace was not yet stabilized and the flux slowly increased with the temperature until a rather stable flux is reached at 2.5×10^{13} atoms/cm^2 s [Fig. 3(b)]. When the K shutter was opened, the substrate temperature was 150 °C [Fig. 3(c)]. The vacuum level increased by several orders of magnitude reaching a stable value of 3×10^{-3} Pa. After 90 min of continuous exposure to K flux, the lock-in amplifier started detecting photocurrent emitted from the cathode surface [Fig. 3(c)]. In 45 min, the QE of the photocathode increased to 0.8%, which is within the range of QEs obtained during this stage of growth when using Bi alloy based dispensers.[10] At this time, the substrate temperature has dropped slightly below 100 °C. The CsN_3 furnace temperature was ramped to 310 °C and the shutter opened to expose the K_3Sb surface to the Cs flux. Contrary to the behavior of previously used K sources, the CsN_3 required more time to reach a stable operations point. As shown in Fig. 3(b), even though the measured furnace temperature was constant, a continuous decrease of the Cs flux was seen, which was compensated by increasing the furnace temperature to 350 °C [Fig. 3(a)]. When the furnace reached this temperature, the flux suddenly increased to 6×10^{13} atoms/cm^2 s [Fig. 3(b)]. At the same time, the substrate temperature was approaching 60 °C, well below the previously reported temperature of 130 °C needed in this stage of the photocathode synthesis while using commercial dispensers. At 60 °C, the substitution reaction, which leads to K loss in favor of Cs incorporation inside the film, proceeded at a very slow rate and the photocurrent, which was so far increasing even with a relatively low rate, started to flatten at a QE of about 2%, indicating that Cs is no longer being incorporated inside the photocathode layer. For this reason, the substrate heater was turned on for the time needed to increase the photocathode temperature above 100 °C [Fig. 3(c)], which according to previous results, is necessary to obtain high QE CsK_2Sb photocathodes.[10] The CsN_3 furnace temperature was decreased to 310 °C as well [Fig. 3(a)], and for the rest of the growth procedure, the generated Cs flux appeared to be constant at 1×10^{13} atoms/cm^2 s [Fig. 3(b)]. The vacuum level stabilized at a 4.5×10^{-3} Pa. As the substrate temperature increased, we observed the QE to rapidly increase and after two more hours of Cs flux exposure the photocurrent flattened at a QE equivalent value of 9.6% for an illuminating wavelength of 532 nm.

IV. SUMMARY AND CONCLUSIONS

This result demonstrates that high quantum efficiency photocathodes based on alkali antimonide materials can be

synthesized using thermal decomposition of alkali azide as sources for the generation of alkali metal vapors. The growth occurs in the presence of relatively high vacuum levels as compared with the process done using alkali chromate or Bi based alloys, but most of the residual gas is high purity nitrogen which does not negatively affect the growth process or contaminate the samples.

Forthcoming experiments will include modifications of the existing apparatus, allowing the exchange of substrate using the same vacuum suitcase and substrate holder used in the ERL injector prototype[17] to measure photocathodes performances in a real photoinjector. We will also attempt the synthesis of Na_2KSb and of the S20 photocathode (which is a Na_2KSb photocathode with a thin Cs_3Sb layer at the top). The latter is known to have a longer wavelength emission threshold. Additionally, we plan a layer-by-layer and coevaporation growth using shutters for precise subnanometer thickness control to study the effect of deposition procedure on the surface roughness and the emission properties.

ACKNOWLEDGMENTS

This work was supported by NSF DMR-0807731 and by DOE DE-SC0003965.

[1]D. H. Dowell *et al.*, Nucl. Instrum. Methods Phys. Res., Sect. A **622**, 685 (2010).
[2]D. H. Dowell, S. Z. Bethel, and K. D. Friddell, Nucl. Instrum. Methods Phys. Res., Sect. A **356**, 167 (1995).
[3]I. V. Bazarov, L. Cultrera, A. Bartnik, B. Dunham, S. Karkare, Y. Li, X. Xianghong, J. Maxson, and W. Roussel, Appl. Phys. Lett. **98**, 224101 (2011).
[4]L. Cultrera, I. Bazarov, A. Bartnik, B. Dunham, S. Karkare, R. Merluzzi, and M. Nichols, Appl. Phys. Lett. **99**, 152110 (2011).
[5]L. Cultrera *et al.*, Phys. Rev. Spec. Top.-Accel. Beams **14**, 120101 (2011).
[6]R. R. Mammei *et al.*, Phys. Rev. Spec. Top.-Accel. Beams **16**, 033401 (2013).
[7]T. Vecchione, I. Ben-Zvi, D. H. Dowell, J. Feng, T. Rao, J. Smedley, W. Wan, and H. A. Padmore, Appl. Phys. Lett. **99**, 034103 (2011).
[8]L. Cultrera, S. Karkare, B. Lillard, A. Bartnik, I. Bazarov, B. Dunham, W. Schaff, and K. Smolenski, Appl. Phys. Lett. **103**, 103504 (2013).
[9]B. Dunham *et al.*, Appl. Phys. Lett. **102**, 034105 (2013).
[10]L. Cultrera *et al.*, *Proceedings of IPAC2012*, New Orleans, Louisiana, 2012, p. 2137.
[11]M. Succi, R. Canino, and B. Ferrario, Vacuum **35**, 579 (1985).
[12]J. Sangster and A. D. Pelton, J. Phase Equilib. **12**, 443 (1991).
[13]I. A. Dubovoi, A. S. Chernikov, A. M. Prokhorov, M. Y. Schelev, and V. K. Ushakov, Proc. SPIE **1358**, 134 (1991).
[14]V. Krishna Mohan and V. R. Pai Verneker, Thermochim. Acta **17**, 343 (1976).
[15]F. Blatter and E. Schumacher, J. Less-Common Met. **115**, 307 (1986).
[16]P. W. M. Jacobs and F. C. Tompkins, Proc. R. Soc. London, Ser. A **215**, 265 (1952).
[17]C. Gulliford *et al.*, Phys. Rev. Spec. Top.-Accel. Beams **16**, 073401 (2013).